PROCEEDINGS OF SCIENCE

Quark-mass Flow of the Nucleon Mass Spectrum in Full QCD

M. S. Mahbub, W. Kamleh, D. B. Leinweber*, P. J. Moran, A. G. Williams
Special Research Centre for the Subatomic Structure of Matter, Adelaide, South Australia 5005, Australia, and Department of Physics, University of Adelaide, South Australia 5005, Australia.

E-mail: md.mahbub@adelaide.edu.au,
waseem.kamleh@adelaide.edu.au,
derek.leinweber@adelaide.edu.au,
peter.moran@alumni.adelaide.edu.au,
anthony.williams@adelaide.edu.au

Our recent first-principles lattice-QCD exploration of the excited states of the nucleon in the positive parity channel is presented. Of particular interest is the first positive-parity excitation of the nucleon; the Roper resonance. Using correlation-matrix methods developed by the CSSM Lattice Collaboration, a low-lying Roper state is observed in our full QCD analysis using the PACS-CS gauge fields made available via the ILDG. A method for tracing the quark-mass flow of energy eigenstates using the eigenvectors of the generalized eigenvalue equations is presented. The results for the Roper display significant curvature as the chiral regime is approached.

XXIX International Symposium on Lattice Field Theory
July 10 – 16, 2011
Squaw Valley, Lake Tahoe, California

*Speaker.

PoS(Lattice 2011)127

1. Introduction

Lattice QCD is a non-perturbative approach to Quantum Chromodynamics (QCD), in fact the only ab initio first principles approach to the fundamental quantum field theory governing the properties of hadrons. While the ground-state hadron spectrum is now well understood, a determination of the excited state energy spectrum is in the process of being revealed with this first principles approach. The results can be compared with the experimental results or provide predictions for future experiments. However, gaining knowledge of the excited-state spectrum presents additional challenges, as the excited energy-states are extracted from the sub-leading exponentials of the correlation functions.

The first positive parity excitation of the nucleon, the $\mathrm{N}\frac{1}{2}^{+}(1440)\,\mathrm{P}_{11}$ or Roper resonance, has been a subject of extensive interest since its discovery in 1964 through a partial-wave analysis of pion-nucleon scattering data [1]. In constituent quark models with a harmonic oscillator potential this P_{11} state (with principal quantum number $\mathrm{N}=2$) appears above the lowest-lying odd-parity S_{11} (1535) state [2, 3], whereas in Nature the Roper resonance is almost 100 MeV below the S_{11} state. Due to its surprisingly low mass, the P_{11} state has held enormous curiosity and speculation in the nuclear and particle physics community. For example, the Roper resonance has been described as a hybrid baryon state with explicitly excited gluon field configurations [4, 5], or as a breathing mode of the ground state [6] or a state which can be described in terms of a five quark (meson-baryon) state [7].

Several attempts have been made in the past to find the elusive low-lying Roper state in the lattice framework, however a low-lying Roper state has not been observed. The difficulties lie in finding effective methods to isolate the energy eigenstates of QCD and in accessing the light quark mass regime of QCD. A recent review of the Roper state can be found in Ref. [8].

The 'Variational method' [9, 10] is the state-of-the-art approach for determining the excited state hadron spectrum. It is based on the creation of a matrix of correlation functions in which different superpositions of excited state contributions are linearly combined to isolate the energy eigenstates. A low-lying Roper resonance was identified with this method using a variety of source and sink smearings in constructing correlation matrices [11, 12] in quenched QCD. Here we bring these effective techniques to the dynamics of full QCD to explore the low-lying even-parity states of the nucleon using 2+1-flavor dynamical QCD gauge-field configurations [13].

Our focus is to present the details of the eigenvector analysis used in reporting our results for the hadron spectrum of full QCD in Ref. [14]. There, a comprehensive analysis of smeared source and sink based correlation matrix constructions formed the foundation of our discovery of a low-lying state associated with the Roper resonance.

2. Variational Method

The variational method is based on the formulation of a correlation matrix. In constructing our correlation matrix for the nucleon spectrum, we consider the two-point correlation function matrix

with momentum $\vec{p} = 0$

$$G_{ij}^{\pm}(t) = \sum_{\vec{x}} \mathrm{Tr}_{\mathrm{sp}} \left\{ \Gamma_{\pm} \langle \Omega | \chi_i(x) \, \bar{\chi}_j(0) | \Omega \rangle \right\}$$
$$= \sum_{\alpha} \lambda_i^{\alpha} \, \bar{\lambda}_j^{\alpha} \, e^{-m_{\alpha} t}, \tag{2.1}$$

where Dirac indices are implicit. Here, λ_i^{α} and $\bar{\lambda}_j^{\alpha}$ are the couplings of the interpolators χ_i and $\bar{\chi}_j$ at the sink and source respectively and α enumerates the energy eigenstates with mass m_{α}. $\Gamma_{\pm} = \frac{1}{2}(\gamma_0 \pm 1)$ projects the parity of the eigenstates.

Since the only t dependence comes from the exponential term, one can seek a linear superposition of interpolators, $\sum_j \bar{\chi}_j u_j^{\alpha}$, such that

$$G_{ij}(t_0 + \triangle t) \, u_j^{\alpha} = e^{-m_{\alpha} \triangle t} \, G_{ij}(t_0) \, u_j^{\alpha}, \tag{2.2}$$

for sufficiently large t_0 and $t_0 + \triangle t$. u_j^{α} are the coefficients multiplying the interpolator $\bar{\chi}_j$ such that state α is created. One can also seek the coefficients v_i^{α} multiplying χ_i to annihilate the state α. This leads to solving right and left eigenvalue equations

$$[(G(t_0))^{-1} \, G(t_0 + \triangle t)]_{ij} \, u_j^{\alpha} = c^{\alpha} \, u_i^{\alpha}, \tag{2.3}$$

$$v_i^{\alpha} \, [G(t_0 + \triangle t) \, (G(t_0))^{-1}]_{ij} = c^{\alpha} \, v_j^{\alpha}. \tag{2.4}$$

The vectors v_i^{α} and u_j^{α} diagonalize the correlation matrix at time t_0 and $t_0 + \triangle t$ providing the eigenstate projected correlator, $v_i^{\alpha} \, G_{ij}^{\pm}(t) \, u_j^{\beta} \propto \delta^{\alpha\beta}$. We define the parity and eigenstate projected correlator

$$G_{\pm}^{\alpha} \equiv v_i^{\alpha} \, G_{ij}^{\pm}(t) \, u_j^{\alpha}, \tag{2.5}$$

which is analyzed using standard techniques to obtain the masses of different energy states.

3. Simulation Details

The PACS-CS $2+1$ flavor dynamical-fermion configurations [13] made available through the ILDG [15] are used in this analysis. These configurations use the non-perturbatively $\mathcal{O}(a)$-improved Wilson fermion action and the Iwasaki-gauge action [16]. The lattice volume is $32^3 \times 64$, with $\beta = 1.90$ providing a lattice spacing $a = 0.0907$ fm.

Five values of the (degenerate) up and down quark masses are considered, with hopping parameter values of $\kappa_{ud} = 0.13700, 0.13727, 0.13754, 0.13770$ and 0.13781, providing pion masses in the range of 702 - 156 MeV; for the strange quark $\kappa_s = 0.13640$. Ensembles of 350 configurations are considered for the four heavier quarks and for the lightest quark an ensemble of 198 configurations is used with a total of 750 fermion sources.

We consider three standard nucleon interpolators $\chi_1(x)$, $\chi_2(x)$ and $\chi_4(x)$ [17]. The correlation matrices are constructed using an extensive sample of different levels of gauge-invariant Gaussian smearing [18] at the fermion source and sink [14]. Among several combinations, a basis of smearing-sweep counts of 16, 35, 100 and 200 is considered as the representative, from which correlation-matrix analyses are performed.

Table 1: The scalar product $\vec{v}^{\alpha}(m_q)\cdot\vec{v}^{\beta}(m_q)$ for $\kappa = 0.13700$ for an 8×8 correlation matrix of χ_1 and χ_2 with four different levels of smearing. States are ordered from left to right and top to bottom in order of increasing excited-state mass.

1.00	-0.09	0.02	0.06	0.65	0.02	-0.31	0.00
-0.09	**1.00**	-0.01	-0.05	-0.06	-0.57	0.03	-0.14
0.02	-0.01	**1.00**	-0.06	0.06	0.05	0.44	-0.02
0.06	-0.05	-0.06	**1.00**	0.12	-0.05	-0.11	0.57
0.65	-0.06	0.06	0.12	**1.00**	0.02	-0.61	0.03
0.02	-0.57	0.05	-0.05	0.02	**1.00**	0.08	0.15
-0.31	0.03	0.44	-0.11	-0.61	0.08	**1.00**	-0.07
0.00	-0.14	-0.02	0.57	0.03	0.15	-0.07	**1.00**

4. Eigenstate Identification

Let us consider M interpolating fields making an $M\times M$ parity-projected correlation matrix $G(t)$. In solving the generalized eigenvalue equations of Eqs. (2.3) and (2.4) we encounter the real and approximately symmetric matrices $[(G(t_0))^{-1}\,G(t_0+\triangle t)]$ and $[G(t_0+\triangle t)\,(G(t_0))^{-1}]$. Thus we expect the eigenvectors of these matrices to be approximately orthogonal.

Using the normalization $\sum_i^M |v_i^{\alpha}|^2 = 1$, we explore the extent to which the eigenvectors $\vec{v}^{\alpha}(m_q)$ for light-quark mass m_q are orthogonal by reporting values for $\vec{v}^{\alpha}(m_q)\cdot\vec{v}^{\beta}(m_q)$ in Table 1. By construction, this quantity is 1 for $\alpha=\beta$ and we observe $\vec{v}^{\alpha}(m_q)\cdot\vec{v}^{\beta}(m_q)$ is significantly different from 1 for $\alpha\neq\beta$.

This feature enables the use of the generalised measure

$$\mathscr{V}^{\alpha\beta}(m_q,m_{q'}) = \vec{v}^{\alpha}(m_q)\cdot\vec{v}^{\beta}(m_{q'}) \tag{4.1}$$

to identify the states most closely related as we move from quark mass m_q to adjacent quark mass $m_{q'}$. Results for this generalized measure of eigenvector overlap are presented in Table 2. For each value of α there is only one value for β where the magnitude of the entry is significantly larger than all others. The most relevant entries for consideration are the immediate neighbours of α where a crossing of the energy levels would move the largest entry off the diagonal. Thus this measure provides a clear identification of how states in the hadron spectrum at quark mass m_q are associated with states at the next value of quark mass, $m_{q'}$.

For each value of α (or β) considered, the entry in the row (or column) with a magnitude closest to one occurrs for $\beta=\alpha$. In this case, there are no level crossings in the spectrum as one moves from quark mass m_q to $m_{q'}$. Level crossings would otherwise reveal themselves as pairs of large-magnitude off-diagonal entries in the matrix.

The values of Table 2 are representative of the values seen for other pairs of quark masses and also for the right eigenvectors $\vec{u}^{\alpha}(m_q)$. Because most of the large entries have a magnitude approaching one, there are typically small changes in the eigenvectors as one moves form one quark mass to the next. Thus, one anticipates a fairly smooth flow of the eigenvector values $\vec{v}^{\alpha}$ as a function of the quark mass.

Table 2: The scalar product $\vec{v}^{\alpha}(m_q) \cdot \vec{v}^{\beta}(m_{q'})$ for $\kappa = 0.13700$ and $\kappa' = 0.13727$ for an 8×8 correlation matrix of χ_1 and χ_2 with four different levels of smearing. States are ordered from left to right for $m_{q'}$ and top to bottom for m_q in order of increasing excited-state mass.

0.97	-0.30	-0.03	-0.27	0.63	0.03	-0.30	0.01
-0.21	**-0.92**	0.17	0.13	-0.04	-0.11	0.44	-0.03
-0.09	0.06	**0.95**	-0.20	-0.06	0.51	0.04	-0.10
0.10	0.03	-0.19	**-0.72**	0.11	-0.28	-0.12	0.59
0.58	-0.46	0.04	-0.45	**0.99**	0.06	-0.60	0.05
0.00	-0.06	-0.40	0.52	0.01	**-0.85**	0.05	0.07
-0.40	-0.13	0.05	0.42	-0.72	-0.20	**1.00**	-0.10
0.04	0.03	-0.17	-0.07	0.04	-0.61	-0.10	**1.00**

5. Quark-mass flow of Eigenvectors and Eigenstates

A key feature of large correlation matrices is the ability to identify and isolate energy eigenstates which are nearly degenerate in energy. However, this approximate degeneracy makes it difficult to trace the flow of states from one quark mass to the next. Thus a clear identification of these near-degenerate states through the features of the eigenvectors isolating the states is necessary in order to trace the propagation of the states from the heavy to the light quark-mass region.

The anticipated smooth flow of the eigenvectors as a function of the quark mass is presented in Fig. 1. It is evident that each energy state has its own eigenvector characteristics. While the quark-mass dependent trends can be significant, they are sufficiently smooth to allow the visual identification of eigenstates at adjacent quark masses. We note that state 1 is the ground state and state 2 is the Roper state.

In Fig. 2, masses are presented for 12 energy eigenstates. The colours and shapes of the symbols identify states having similar eigenvectors as illustrated in Fig. 1. While the eigenvectors for the first excited state (state 2 in Fig. 1) have a significant quark-mass dependence that is smoothly varying over the quark mass range considered, the baryon masses obtained for this state do not vary smoothly. For the two large quark masses, the results sit close to the P-wave $N\pi$ scattering threshold whereas the masses for the lighter three quark masses sit much higher.

A possible explanation for this feature is that the attractive mass-dependent and spin-dependent forces which are necessary for the formation of a strong resonance only have sufficient strength at light quark masses. For example, it is typical to encounter spin-dependent forces which are inversely proportional to the product of the quark masses undergoing gluon exchange. At light quark masses, resonances dominate the spectral function whereas at heavy quark masses, only the multiparticle states have spectral strength sufficient to be seen in the spectrum.

Future calculations should investigate the use of five-quark operators to better explore overlap with the multiparticle states in the light quark-mass region. Already, novel work using the stochastic LapH method is in progress [19]. It will also be interesting to explore the first excited state on a large volume lattice to better understand the relationship between this state with its neighbouring scattering states.

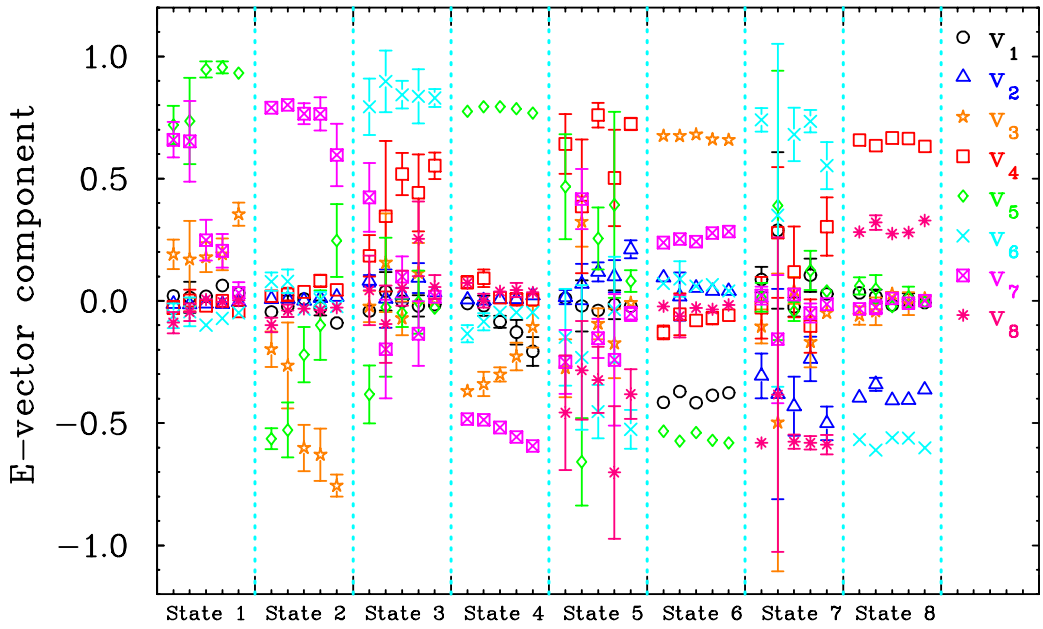

Figure 1: (Color online). Eigenvector components for the five different quark masses are presented after identifying eigenstates via $\vec{v}^{\alpha}(m_q) \cdot \vec{v}^{\beta}(m_{q'})$. For each energy eigenstate, the eigenvector components are plotted in order of increasing quark mass. In the legend, (v_1, v_2), (v_3, v_4), (v_5, v_6) and (v_7, v_8) correspond to the smearing-sweep levels of 16, 35, 100 and 200 respectively. Odd numbers in the subscripts of v correspond to the contribution from the χ_1 interpolator, whereas, even numbers correspond to χ_2. Similar results are observed for the right eigenvectors.

6. Acknowledgments

We thank PACS-CS Collaboration for making these 2+1 flavor configurations available and the ILDG for creating the opportunity, tools and formalism for sharing these configurations. This research was undertaken on the NCI National Facility in Canberra, Australia, which is supported by the Australian Commonwealth Government. We also acknowledge eResearch SA for grants of supercomputing time which have enabled this project. This research is supported by the Australian Research Council.

References

[1] L. D. Roper, Phys. Rev. Lett. 12 (1964) 340–342.

[2] N. Isgur, G. Karl, Phys. Lett. B72 (1977) 109.

[3] N. Isgur, G. Karl, Phys. Rev. D19 (1979) 2653.

[4] Z.-p. Li,V. Burkert, Z.-j. Li, Phys. Rev. D46 (1992) 70–74.

[5] C. E. Carlson, N. C. Mukhopadhyay, Phys. Rev. Lett. 67 (1991) 3745–3748.

[6] P. A. M. Guichon, Phys. Lett. B164 (1985) 361.

[7] O. Krehl,C. Hanhart,S. Krewald, J. Speth, Phys. Rev. C62 (2000) 025207. [arXiv:nucl-th/9911080]

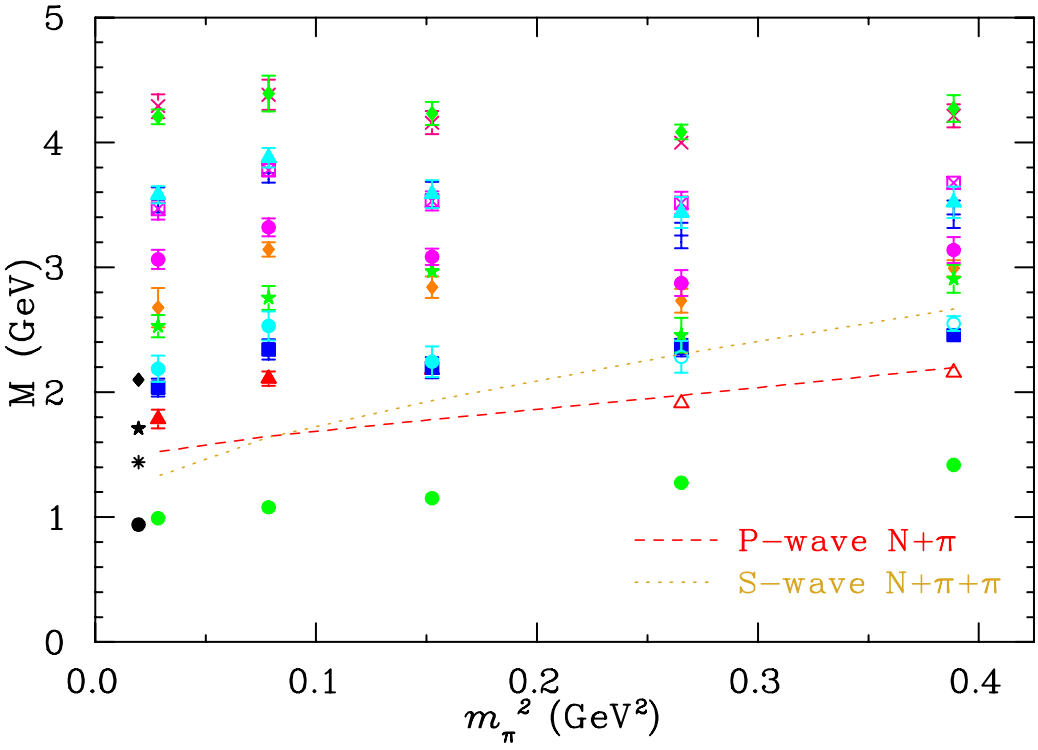

Figure 2: (Color online) Masses of the positive-parity energy-states of the nucleon. The colours and shapes of the plotting symbols are used to identify states having similar eigenvectors as illustrated in Fig. 1. Physical values [20] and plotted at the far left. Lattice results for the Roper (red triangles) reveal significant chiral curvature towards the physical mass. The P-wave $N\pi$ scattering threshold (with one unit of lattice momentum) and the S-wave $N\pi\pi$ threshold are presented by dashed and dotted lines, respectively.

[8] H.-W. Lin, S. D. Cohen. [arXiv:1108.2528].

[9] C. Michael, Nucl. Phys. B259 (1985) 58.

[10] M. Luscher, U. Wolff, Nucl. Phys. B339 (1990) 222–252.

[11] M. S. Mahbub, et al., Phys. Lett. B679 (2009) 418–422. [arXiv:0906.5433].

[12] M. S. Mahbub,A. O. Cais,W. Kamleh,D. B. Leinweber, A. G. Williams, Phys. Rev. D82 (2010) 094504. [arXiv:1004.5455].

[13] S. Aoki, et al., Phys. Rev. D 79 (2009) 034503. [arXiv:0807.1661].

[14] M. S. Mahbub,W. Kamleh,D. B. Leinweber,P. J. Moran, A. G. Williams. [arXiv:1011.5724].

[15] M. G. Beckett, et al., Comput. Phys. Commun. 182 (2011) 1208–1214. [arXiv:0910.1692].

[16] Y. IwasakiUTHEP-118.

[17] D. B. Leinweber,R. M. Woloshyn, T. Draper, Phys. Rev. D43 (1991) 1659–1678.

[18] S. Gusken, Nucl. Phys. Proc. Suppl. 17 (1990) 361–364.

[19] C. Morningstar, et al., Phys. Rev. D83 (2011) 114505. [arXiv:1104.3870].

[20] C. Amsler, et al., Phys. Lett. B667 (2008) 1.